A POTENTIAL FIELD MODEL FOR OPEN FIELD LINES IN THE ACTIVE REGION CORONA

T. Sakurai

National Astronomical Observatory, Mitaka, Tokyo 181, Japan

Abstract

An extention of the conventional source surface model is constructed by using the Green's function method for potential magnetic fields. The method is applied to simple configurations such as dipole fields to examine the performance of the proposed method. Then the method is applied to a real magnetogram and the result is compared with observed structures in the corona.

1. Introduction

For given magnetic data B_b on the solar surface, one can compute the potential magnetic field $\boldsymbol{B} = -\nabla\phi$ by using the Green's function method

$$\phi(r) = \int G(\boldsymbol{r}, \boldsymbol{r}') B_b(\boldsymbol{r}') d\boldsymbol{S}'. \tag{1}$$

The effect of the solar wind is taken into account by using the so-called source surface approximation, in which the field lines are assumed to be radial at a radius $r = r_s$. This can be accomplished by a proper choice of Green's function, although the field vector at the source surface can only be made approximately radial.

In the conventional source surface models, the data are accumulated over one solar rotation. Such models are intended to deal with magnetic structures whose life time is as long as one month. Our approach is to apply the source surface concept in a localized region. Instead of accumulating data over one solar rotation, we only work on a single magnetogram. The invisible solar hemisphere is assumed to be either field-free, or to be the mirror reflection of the visible hemisphere.

2. Green's Functions

Here we consider two kinds of Green's functions, G_n and G_l. If the given data are the normal components of the magnetic field on the solar surface (B_n), Green's function to be used is G_n which was derived by Sakurai (1982). When using this Green's function, the

invisible hemisphere is assumed to be field-free. If the observed region is not at the disk center, the quantity B_n is not generally derived from a longitudinal magnetogram. The component B_n can be deduced from a vector magnetogram, if it is available.

If the given data are the longitudinal components of the magnetic field (B_l), Green's function in this case (G_l) was given by Sakurai (1993). This Green's function was derived by assuming that the line-of-sight component of the field is anti-symmetric with respect to the plane of the sky. In conformity with this assumption, the data should be extended into the invisible hemisphere as the mirror reflection of the visible hemisphere.

3. Example-1: Dipole Field

In order to confirm the performance of our schemes, we first generated magnetic maps of B_n and B_l corresponding to a dipole magnetic field. Then we applied two kinds of Green's function methods to the simulated magnetograms. Fig.1a,b show the dipole field reconstructed by using G_n: The source surface is not taken into consideration in Fig.1a. Fig.1b corresponds to the case of $r_s = 2r_\odot$.

Fig.2a,b show the dipole field reconstructed by using G_l: The source surface is not taken into consideration in Fig.2a. Fig.2b corresponds to the case of $r_s = 2r_\odot$. The field lines are symmetric with respect to the plane of the sky.

The actual deviation of the field from the radial direction on the source surface depends on the boundary data. It was found from many runs of simulations that the deviation is larger for G_l than for G_n. The advantage of G_l in that it does not require vector magnetic data is offset by its lower accuracy of the field directions on the source surface.

4. Example-2: A Realistic Application

Next we examined our procedure on a real magnetogram. A large limb flare with a developed Hα loop prominence system was observed on 1992 November 2 with the Solar Flare Telescope at Mitaka (Ichimoto et al., 1993). The Solar Flare Telescope also obtained vector magnetograms of this active region on October 28, when the region was still on the disk (fig.3). The magnetic field vectors were highly sheared along the north-eastern magnetic neutral line, on which the loop prominence system of November 2 was located. We computed field lines based on the vector magnetogram shown in fig.3, by using Green's function G_n with $r_s = 1.25r_\odot$. The field lines thus obtained were then rotated westward by the difference of the time between the flare and the magnetographic observation (fig.4). The fit is not very satisfactory, and apparently the shear in the magnetic field along the neutral line remained in the post-flare arcade.

One often sees cusp-shaped loops in soft X-ray images of Yohkoh (Acton et al., 1992). Our next plan is to apply the present method to active regions showing such cusp structures, and to see whether the cusp structures represent an open field configuration or are merely due to the projection effect.

References

1. Acton, L.W., et al., 1992, *Science*, **258**, 618.
2. Ichimoto, K., et al., 1993, in *Proceedings of Japan-China Workshop on Solar Physics*, eds. T.Sakurai, T.Hirayama and G.Ai, National Astronomical Observatory, in press.
3. Sakurai, T., 1982, *Solar Phys.* **76**, 301.
4. Sakurai, T., 1993, *IAU Colloq.* **141**, p.91.

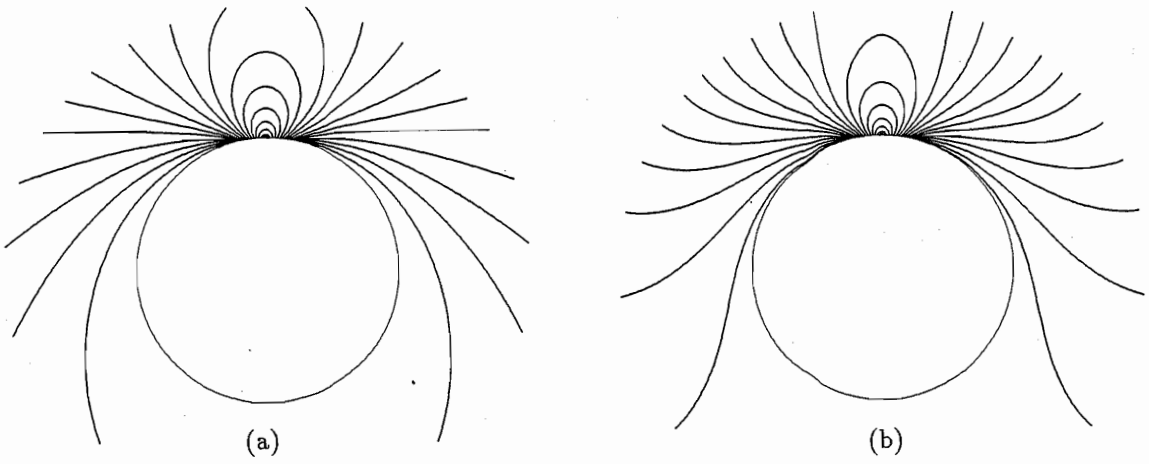

Fig. 1. Dipole field lines reproduced by G_n, with (a) $r_s = \infty$, and (b) $r_s = 2r_\odot$.

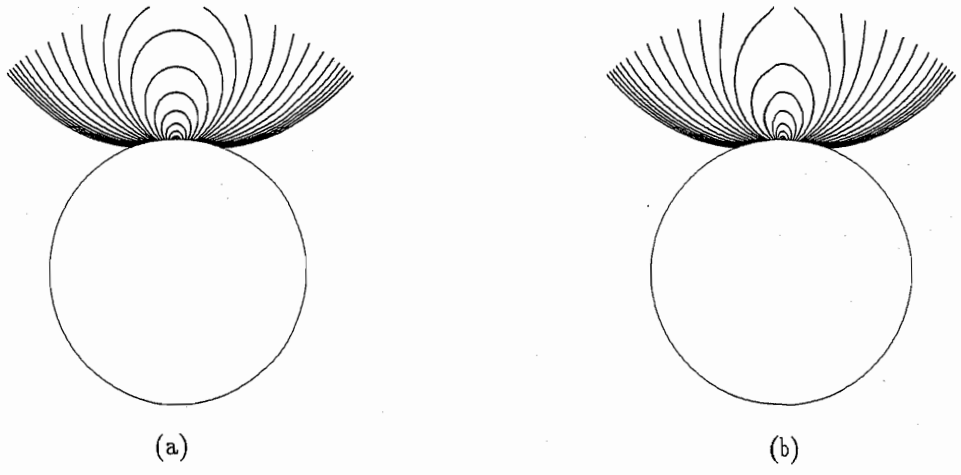

Fig. 2. Dipole field lines reproduced by G_l, with (a) $r_s = \infty$, and (b) $r_s = 2r_\odot$. The line-of-sight direction is up.

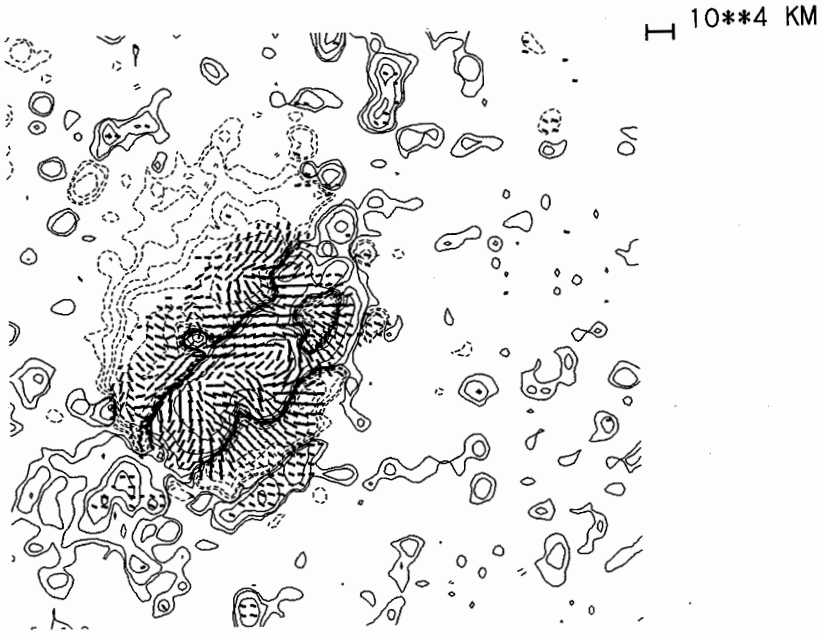

Fig. 3. A vector magnetogram of 1992 October 28, obtained with the Solar Flare Telescope at Mitaka.

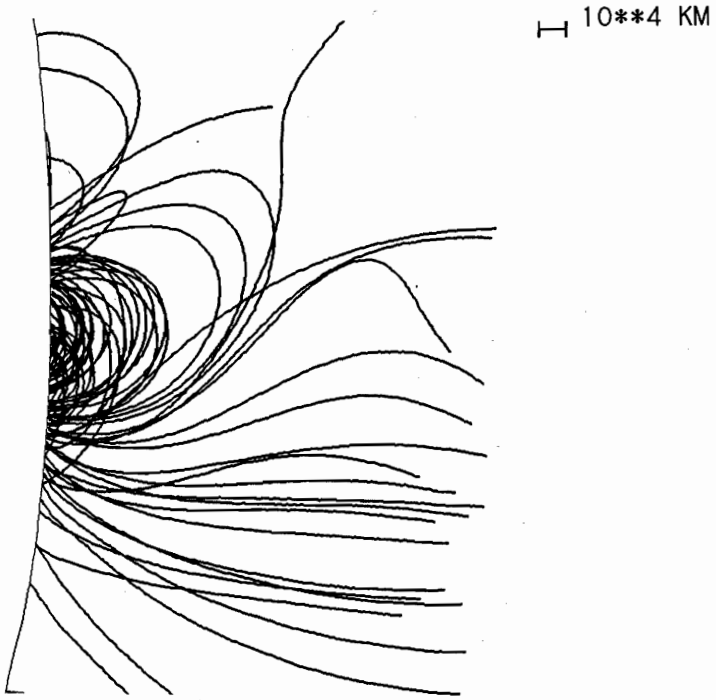

Fig. 4. Field lines calculated based on the vector magnetogram of fig.3, rotated by 68° westward to simulate the time of the flare of 1992 November 2. Green's function G_n with $r_s = 1.25 r_\odot$ was used.